Modified oil palm leaves adsorbent with enhanced hydrophobicity for crude oil removal

S.M. Sidik [a], A.A. Jalil [b,*], S. Triwahyono [a], S.H. Adam [b], M.A.H. Satar [b], B.H. Hameed [c]

[a] Ibnu Sina Institute for Fundamental Science Studies, Faculty of Science, Universiti Teknologi Malaysia, 81310 UTM Johor Bahru, Johor, Malaysia
[b] Institute of Hydrogen Economy, Faculty of Chemical Engineering, Universiti Teknologi Malaysia, 81310 UTM Johor Bahru, Johor, Malaysia
[c] School of Chemical Engineering, Engineering Campus, Universiti Sains Malaysia, 14300 Nibong Tebal, Penang, Malaysia

HIGHLIGHTS

▶ A new low-cost biodegradable oil adsorbent was developed from oil palm leaves (OPLs).
▶ Lauric acid enhanced the hydrophobicity and adsorption ability of OPL.
▶ The adsorption was controlled by film-diffusion mechanism.
▶ Maximum adsorption capacity was 1176 ± 12.92 mg g^{-1} at optimized conditions.
▶ The OPL$_{LA}$ has the potential of removing crude oil from oily water mixture.

GRAPHICAL ABSTRACT
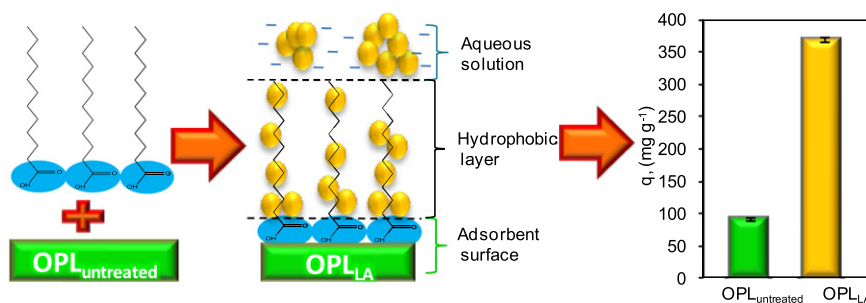
ABSTRACT

The removal of crude oil from water by lauric acid (LA) modified oil palm leaves (OPLs$_{LA}$) was investigated by batch adsorption after varying pH (2–11), contact time (10–60 min), adsorbent dosage (0–52 g L^{-1}), initial oil concentration (0–6400 mg L^{-1}) and temperature (303–323 K). The modification significantly increased the hydrophobicity of the adsorbent, thus creating OPL$_{LA}$ with much better adsorption capacity for crude oil removal. The results gave the maximum adsorption capacity of 1176 ± 12.92 mg g^{-1} at 303 K. The significant uptake of crude oil from water was proven by FT-IR and FE-SEM analyses. The isotherms studies revealed that the experimental data agrees with the Freundlich isotherm model. The pseudo-second-order kinetics model fitted well the experimental results. Boyd's and Reichenberg's equation on adsorption dynamic revealed that the adsorption was controlled by internal transport mechanism and film-diffusion was the major mode of adsorption. The prepared adsorbent showed the potential to use as a low-cost adsorbent in oil-spill clean-up.

© 2012 Elsevier B.V. All rights reserved.

1. Introduction

Massive oil spills have occurred frequently as a result of human mistakes and carelessness, deliberate acts (i.e. war and vandalism) and natural disasters (i.e. earthquakes and hurricanes) [1]. These incidents resulted in a great deal of damage to the human health quality, serious environmental pollution and loss in the huge amount of petroleum energy source [2]. Therefore, it is essential to collect and clean the oil promptly after a spillage.

Advanced removal and recovery of oil by oil sorbent materials is of great interest from economical and ecological standpoints and therefore, various materials have been applied to this end [3]. These studies almost exclusively use either inorganic mineral materials, organic synthetic product or organic natural materials as the adsorbent [4]. Recently, the use of various types of natural organic adsorbents [2,5–11] is particularly interesting because of their greater adsorption capacities, higher biodegradability and

* Corresponding author. Tel.: +60 7 5535581; fax: +60 7 5536165.
  E-mail address: aishah@cheme.utm.my (A.A. Jalil).

cost effectiveness compared to the inorganic and synthetic organic adsorbents that are normally used. However, abundant and locally available adsorbents with a good oil-sorption capacity are still in need.

The local oil-palm industry is estimated to generate 30 million tons of a lignocellulosic biomass per year in the form of trunks, fronds, empty fruit bunches and leaves [12]. These wastes are not being utilized effectively; land filling and open burning are common practices to eliminate these oil-palm residues, and these methods can cause pollution that adversely impacts the ecosystem [13]. Therefore, finding uses for these abundant biomasses, especially on a large scale, would be profitable from both an environmental and an economic point of views.

Therefore, herein we chose oil-palm leaves (OPLs) as a model adsorbent and studied their potential for removing crude oil from water. OPL was reported to consist of 47.7% holocellulose, 44.53% α-cellulose and 27.35% lignin [14]. Due to the availability of the specific functional groups such as hydroxyl (—OH) groups in the OPL, the surface characteristics of the OPL can be modified to improve its adsorption properties. Several studies have been conducted for the surface modifications of agricultural waste/byproduct [15,16], but the use of less expensive fatty acids as the modification agent is still rare.

In the present study, the influence of surface modification on adsorption performance were evaluated for the removal of crude oil under various experimental conditions of pH, adsorbent dosage, contact time, initial oil concentration and temperature. A few attempts have been made in studying the engineering aspects of the adsorption mechanism such as kinetics, equilibrium and thermodynamics of the adsorption of crude oil onto OPL_{LA}.

2. Material and methods

2.1. Materials

The mature OPL were collected from the Johor oil-palm plantation, Malaysia. The crude oil was obtained from petroleum plant station, Kerteh, Malaysia and used as received. The oily-water mixture was prepared at the desired concentration using Milli-Q water.

2.2. Preparation of adsorbent

The green-colored OPL were cut into small pieces to obtain suitably sized OPL for blending. The pieces were washed with water to remove any adhering substances and were then oven-dried at 353 K. The pieces were then ground and sieved to a constant size of 355–500 μm and oven-dried at 373 K for 24 h to a constant weight before being stored in a plastic bottle. The uniformity of OPL particles in this size range led to a well-mix during the adsorption.

Treated OPL was prepared by suspending 2 g of powdered OPL in 200 mL of 1.0 M lauric acid solution. The mixture was stirred for 6 h at room temperature and then filtered. The resultant adsorbent sample was washed with n-hexane several times before being oven-dried overnight at 353 K. Weight percent gain (WPG) of the OPL due to the modification with lauric acid was calculated according to:

$$WPG(\%) = \left[\frac{Weight\ gain}{Original\ weight}\right] \times 100 \qquad (1)$$

The hydrophobicity degree (HD) of the OPL and OPL_{LA} were defined as the tendency of the materials to be removed from the water phase into a non-polar phase. In this experiment, 1.0 g of adsorbent was placed in a beaker with 20 mL of water and with sufficient agitation. Following this, hexane with the same volume of water was added to the beaker and agitated for 3 min. The mixture was then let to stand for 5 min for the separation of the two immiscible phases. The quantity of the adsorbent transferred to the organic phase was determined by filtration and subsequent drying and weighing. The results are expressed in term of the percent of adsorbent transferred into the organic phase. The values of the percent proportion used as the estimations of the degree of hydrophobicity of the adsorbent were calculated based on the following equation:

$$HD(\%) = \left[\frac{Weight\ of\ adsorbent\ in\ hexane}{Original\ weight}\right] \times 100 \qquad (2)$$

2.3. Characterization of crude oil and OPL

The hydrocarbon content in the crude oil before and after 7 days of exposure under sunlight was analyzed using a gas chromatograph equipped with a mass spectrometer detector (GC–MS, Hewlett Packard HP 5890A-Series II, USA). The infrared spectra of the OPL sample were obtained using a Fourier-transform infrared spectrometer (FT-IR, Spectrum GX, Perkin Elmer, USA). The samples were prepared as KBr pellets and scanned over the range of 400–4000 cm^{-1} to identify the functional groups that were responsible for adsorption. The surface morphology of the OPL before and after adsorption was examined using a field-emission scanning electron microscope (FE-SEM, JEOL JSM 6710F). The surface area of the adsorbents was measured using surface analyzer (Quantachrome Autosorb-1 analyzer) by BET method.

2.4. Adsorption experiments

Adsorption experiments were performed by adding 1 g of OPL in a 50 mL conical flask containing 25 mL of a 2400 mg L^{-1} oil mixture. The pH of the working mixtures was adjusted to the desired value with 0.1 M HCl or NaOH. The mixtures were prepared under constant stirring at a rate of 300 rpm at room temperature (303 K) to reach equilibrium. The samples were then withdrawn at appropriate time intervals and centrifuged at 3500 rpm for 15 min. The supernatant was filtered using a Millex-HN filter (Millipore, 0.45 μm), and the oil left at the top of the mixture was extracted using n-hexane. The residual oil concentration was determined using a double-beam UV/vis spectrophotometer (Thermo Scientific Genesys 10UV Scanning) at 280 nm. All experiments were performed in triplicate. Statistical analysis was carried out by comparing means of each crude oil removals using one-way analysis of variance.

At any time, t, the adsorption uptake of oil adsorbed (q_t, mg/g) on OPL was calculated by the following mass-balance equation:

$$Adsorption\ uptake,\ q_t = \left(\frac{C_0 - C_t}{m}\right) V \qquad (3)$$

where C_o and C_t (mg/L) are the liquid-phase concentrations of the oil at the initial and at time t, respectively, V (L) is the volume of the mixture and m (g) is the mass of OPL used.

3. Results and discussion

3.1. Characterizations of the adsorbent

3.1.1. Functional groups identification

The determination of the chemical structure of OPL before and after pretreatment, as well as before and after adsorption, could verify the possible functional groups involved in its binding mechanism between lauric acid and oil. Fig. 1 shows the FTIR spectra of
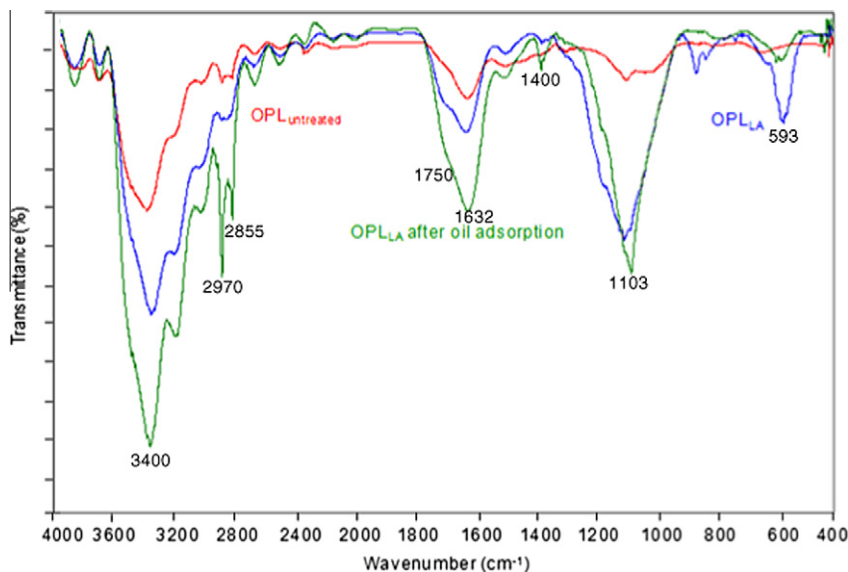
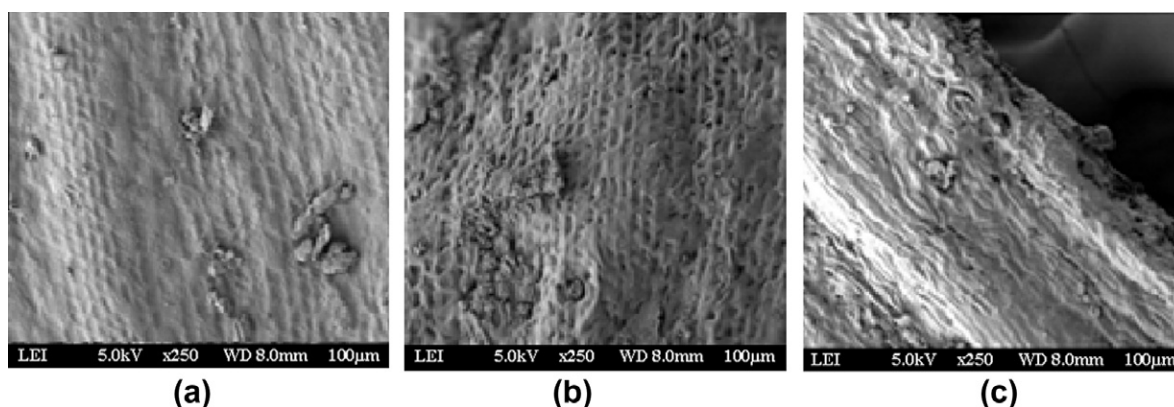**Fig. 1.** FTIR spectra of OPL_untreated, OPL_LA and OPL_LA after oil adsorption.

Fig. 2. FE-SEM images of (a) OPL_untreated, (b) OPL_LA and (c) OPL_LA after oil adsorption. (Magnification: 250×).

OPL_untreated, OPL_LA and OPL_LA after oil adsorption. A strong band at 3400 cm^{-1} is attributed to the intra- and inter-molecular hydrogen-bonded (O—H) stretching that occurs in cellulose. Two peaks observed between 2970 and 2855 cm^{-1} were assigned to the presence of C—H asymmetric stretching of CH$_3$ and CH$_2$ groups [17]. The presence of a peak observed at 1750 cm^{-1} is attributed to the C=O stretching of the carbonyl group [18]. The vibration of C=C stretching mode was observed at 1632 cm^{-1}, may be attributed from aromatics of both OPL and the crude oil. The band at 1400 cm^{-1} may represent the C—H bending vibration mode [19]. The broad peaks at approximately 1103 and 1060 cm^{-1} show the C—O—C stretching vibration of lignin and the C—O stretching of cellulose and hemicellulose, respectively [20].

The increase in the peak intensity of CH$_3$ and CH$_2$ groups after the treatment of OPL with lauric acid has suggested the successful impregnation of lauric acid into the OPL. This hypothesis was confirmed with the presence of a new peak at 1750 cm^{-1}, corresponding to the carbonyl group originated from the lauric acid chain. This result is in good agreement with the improvement of the hydrophobicity degree of the OPL from 16.3% to 84.7% after the treatment. In addition, it was supported with the increment in the weight of OPL after the treatment with WPG is about 4.62%. It is suggested; the increased in the hydrophobicity of OPL after modification with LA will increase the affinity of OPL_LA to absorb more crude oil.

The attachment of crude oil onto the surface of OPL_LA was observed at 2970 and 2855 cm^{-1}; where the peaks become more intensified after the adsorption process. A well-pronounced trough at 1632 cm^{-1} which is associated with the presence of C=C stretching of aromatics of the crude oil was increased significantly after the crude oil adsorption. The adsorption of crude oil was further evidenced by the presence of a new peak at 1400 cm^{-1} after the adsorption which represents the C—H bending of crude oil. The C—H deformation band at 593 cm^{-1} decreased in intensity after the adsorption, possibly because of the interaction of the lauric acid chain with the petroleum hydrocarbons.

3.1.2. Morphology identification

The FE-SEM images of OPL before and after the pretreatment with lauric acid and also after oil sorption were showed in Fig. 2. The smoother surface of OPL became corroded and coarse with a highly porous texture after the pretreatment, suggesting the removal of waxy cuticle layer of the OPL during the modification, thus increased contact area for the adsorption of oil. Following crude oil adsorption, the pores of OPL_LA were filled and adhered with oil, which covered the surface of the OPL_LA with a series of irregular oil cavities. The irregular surfaces implied the adsorption of crude oil onto the OPL_LA.
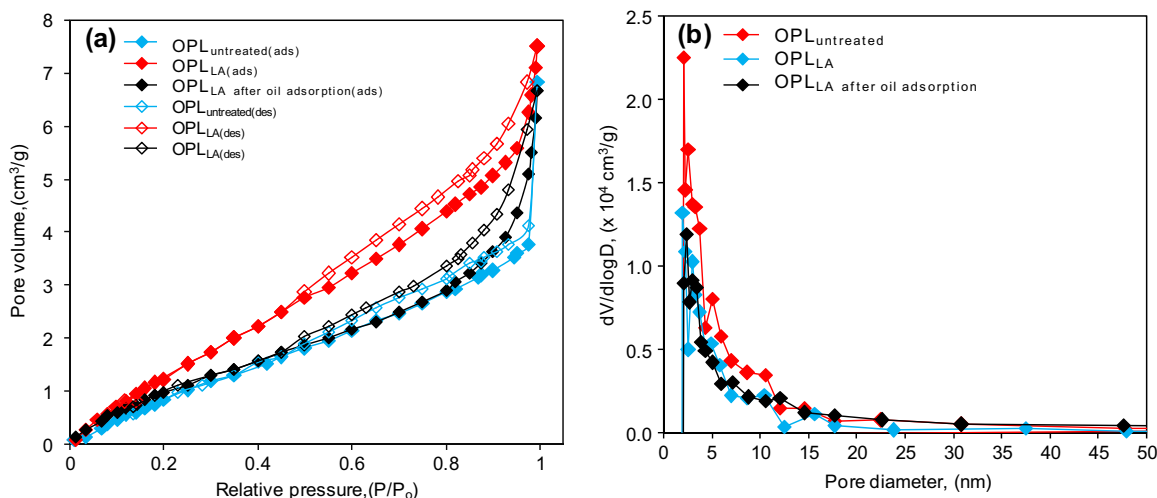
Fig. 3. Nitrogen adsorption–desorption isotherms and pore size distributions of $OPL_{untreated}$, OPL_{LA} and OPL_{LA} after oil adsorption.
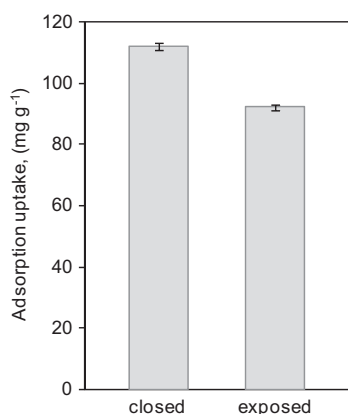

Fig. 4. Effect of hydrocarbon fraction of crude oil on adsorption onto $OPL_{untreated}$. (pH 7, 2400 mg L^{-1} oil, 40 g L^{-1} OPL_{LA}, 60 min, 303 K).

3.1.3. Textural properties identification

Nitrogen sorption measurements were conducted to further characterize the pore parameter of the adsorbents. The obtained nitrogen adsorption–desorption and pore size distribution are shown in Fig. 3a and b, respectively. In accordance with the IUPAC classification, all the adsorbents showed a typical type II adsorption–desorption isotherm, indicating the presence of mesopore [21]. From the physical parameters obtained from the N_2 adsorption isotherm, it is evident that the modification of $OPL_{untreated}$ with lauric acid increased the surface area and pore volume of the OPL_{LA}. Thus, possibly enhances the ability of the adsorbent for trapping oil and also facilitate the pore distribution during adsorption. It is noted, the OPL_{LA} after oil adsorption has slightly decreased in surface area and pore volume due to the oil pore-blocking effect.

The structural heterogeneity is generally characterized in terms of pore size distribution [22]. The pore size distribution curves showed a few peak detected, with the sharpest peak occurred at pore diameter between 2–2.3 nm for all adsorbents. The average pore sizes of $OPL_{untreated}$, OPL_{LA} and OPL_{LA} after oil adsorption were 3.87 nm, 4.93 nm and 5.86 nm, respectively.

In overall, the BET analysis shows no significant changes in the surface area, pore volume and pore diameter for the $OPL_{untreated}$, OPL_{LA} and OPL_{LA} after crude oil adsorption. Therefore, we suggested that surface area gave less contribution for the crude oil adsorption compared to the hydrophobicity as mentioned before in Section 3.1.1.

3.2. Effect of hydrocarbon fraction in crude oil

To study the capability of OPL_{LA} to adsorb petroleum hydrocarbons with various fractions, the oil that was exposed for 7 days to air was used and compared with fresh crude oil obtained from the plant station (closed oil). As can be seen from Fig. 4, the adsorption uptake of closed oil is slightly higher than that of the exposed oil, which indicates that the OPL_{LA} adsorbed closed oil more easily than exposed oil. This result may be explained by the GC–MS chromatograms shown in Fig. 5. After being exposed for 7 days, the lighter hydrocarbons evaporated and the viscosity of the oil increased, which resulted in the deceleration of the oil diffusion into the internal surface of the OPL_{LA}. A similar observation has been reported for the removal of oil by walnut-shell media [23]. However, the lighter hydrocarbons of closed crude oil that adhered to the surface of the OPL_{LA} were expected to desorb more easily during centrifugation than the heavy hydrocarbons in exposed crude oil due to the weaker binding strength of crude oil to OPL [24]. Overall, only minor differences were observed in both the adsorption uptake and the removal percentage of the closed and exposed oil onto the OPL_{LA}. Therefore, the exposed oil was used for further investigations to combine the advantages of applying the spilt-oil conditions.

3.3. Effect of pretreatment of OPL

Preliminary study was conducted by using $OPL_{untreated}$ as an adsorbent to remove crude oil from aqueous mixture. However, the $OPL_{untreated}$ was found to show poor efficiency for crude oil removal with the adsorption uptake of 92.32 ± 2.54 mg g^{-1}. This was expected as raw agricultural waste usually exhibited low sorption capacity due to the presence of many hydroxyl groups on its surface. The presents of hydroxyl groups on the surface of $OPL_{untreated}$ is hypothesized to repel the crude oil molecules in the adsorption medium, thus reduced the adsorption uptake [25].

The effectiveness of lauric acid in increasing the affinity of OPL to adsorb oil was proven with the increase in the adsorption uptake of OPL up to 369.60 ± 3.43 mg g^{-1}. A proposed mechanism in Fig. 6 was used to explain the results. The introduction of the lauric acid chain to the $OPL_{untreated}$, which is rich with hydroxyl groups of cellulose, hemicelluloses and lignin, promotes an esterification process to occur [26]. The substitution of hydroxyl groups with the alkyl chain from the lauric acid has lead to the creation of a non-polar layer on the OPL_{LA} surface. The increase in the hydro-
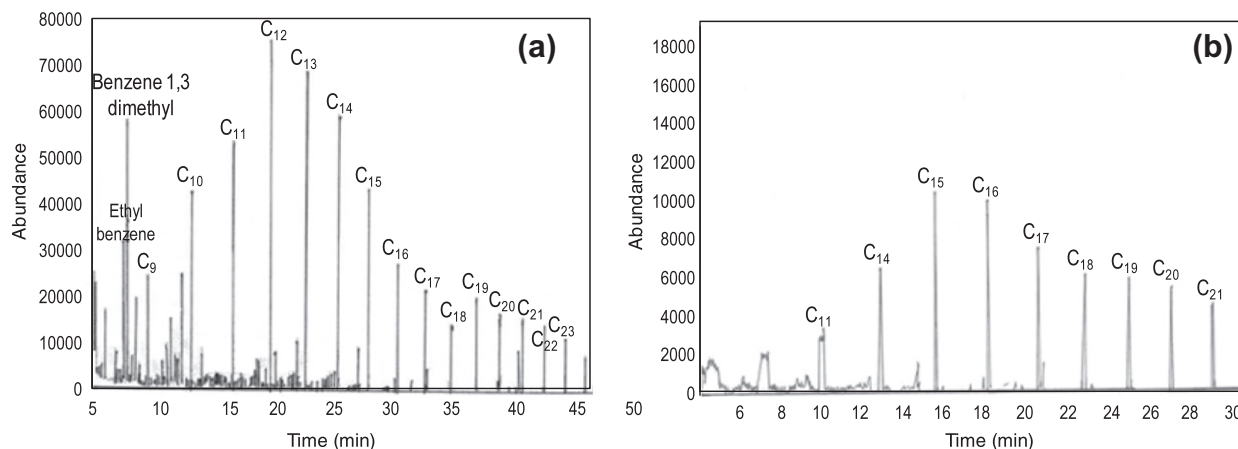
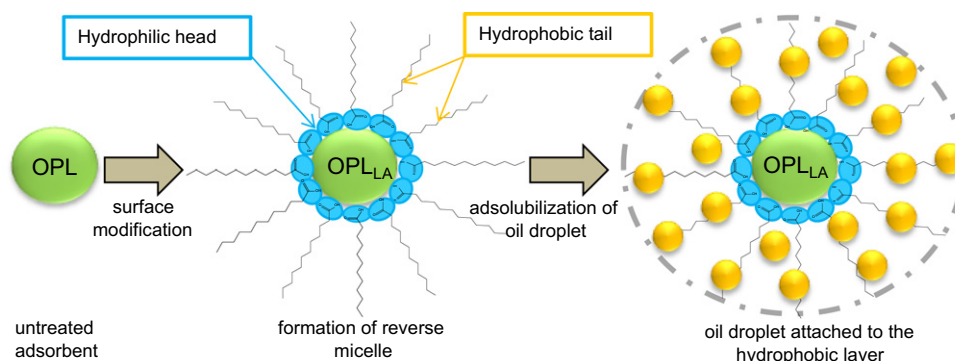**Fig. 5.** GC–MS chromatograms of (a) closed and (b) exposed crude oil.

Fig. 6. Proposed mechanism of oil adsorption onto OPL$_{LA}$.

phobicity degree and the contact area of the OPL$_{LA}$ was believed to enhance and provided more superior sites for higher oil adsorption uptake.

3.4. Effect of pH

The initial pH of the mixture is a vital process parameter for controlling the adsorption because the aqueous chemistry and surface binding sites of the adsorbent are dependent on the pH value of the mixture [27]. Herein, the effect of initial pH of the oil mixture on the adsorption process was studied in the range of 2–12 (Fig. 7). The adsorption uptake at the mixture pH 2 until 9 increased dramatically from 360.63 ± 0.27 to 370.18 ± 0.63 mg g^{-1}. However, in the pH range of 9–2, the adsorption uptake was almost the same as in the range of 370.18 ± 0.63 to 370.65 ± 0.56 mg g^{-1}. This variation can be explained by the change in the amounts of protons and hydroxyl ions present in the mixture.

At low pH, huge amounts of protons were available in the mixture and they saturated the adsorbent sites. As a result, the cationic properties of the adsorbent surface were increased [28]. This phenomenon can greatly reduce the hydrophobic properties of the adsorbent, thus severely affecting the performance of OPL$_{LA}$ for crude oil uptake. In addition, it was suggested that strong acidity can cause coalescence and induce in the increase of crude oil droplet size [28]. These crude oil droplets in the hydrophobic layer are expected to experience severe stress and can be easily desorbed from the adsorbent [26].

The highest adsorption uptake was observed at high pH. However, this did not correspond to the crude oil removal efficiency but the addition of sodium hydroxide (NaOH) for alkaline pH
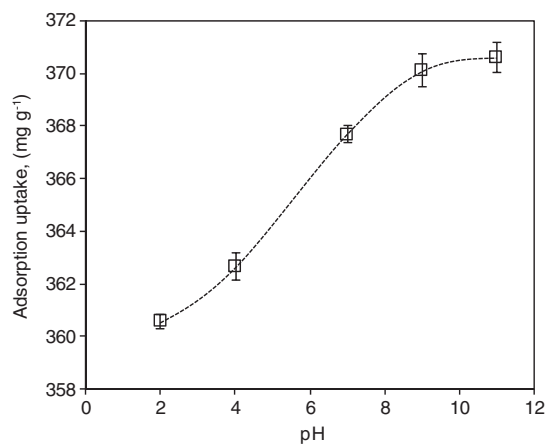

Fig. 7. Effect of pH on adsorption of crude oil onto OPL$_{LA}$. (2400 mg L^{-1} exposed oil, 40 g L^{-1} OPL$_{LA}$, 60 min, 303 K).

adjustment which resulted in the saponification process to occur [28]. When NaOH was added, the crude oil reacted or undergo hydrolysis with the NaOH to produce glycerol and fatty acid salts, called soap. The resultant compound was more soluble in water than in hexane. Therefore, when determining the final crude oil concentration of the treated sample, the crude oil concentration was found to be lower at pH 9 and 12, since the crude oil was hydrolyzed in the aqueous mixture and was not being extracted into the hexane.
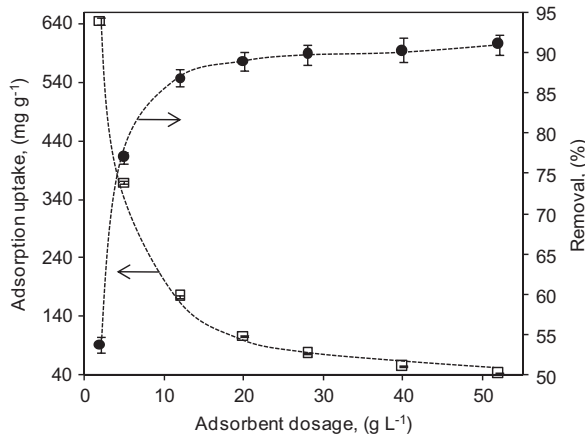
Fig. 8. Effect of adsorbent dosage on adsorption of oil onto OPL$_{LA}$. (pH 7, 2400 mg L^{-1} exposed oil, 60 min, 303 K).

Fig. 9. Isotherm plots for crude oil adsorption onto OPL$_{LA}$.

Thus, as shown in Fig. 7, the optimum pH for adsorption of crude oil from aqueous mixture by OPL$_{LA}$ was at 7 and the adsorption uptake was 367.73 ± 0.34 mg g^{-1}. The condition seems to be advantageous for crude oil spill treatment since the pH of seawater falls within the range of 6–9. Furthermore, this gives an advantage to the treatment process whereby the final discharge after adsorption will have neutral pH. For this reason, no further adjustment of pH would be required after the adsorption before the effluent could be discharged.

3.5. Effect of adsorbent dosage

The effect of adsorbent dosage on the amount of crude oil removed was studied by the application of dosage between 2 and 52 g L^{-1}. As can be seen in Fig. 8, the removal of crude oil was observed to be dependent on the dosage of OPL$_{LA}$. The rate of removal percentage increased instantaneously with increasing adsorbent dosage from 2 to 52 g L^{-1}, and then gradually decreased until the equilibrium was achieved when the efficiency of crude oil removal was 91.00 ± 1.31%. In contrast, the adsorption uptake increased with decreasing OPL$_{LA}$ dosage, and the maximum sorption capacity of 645.73 ± 6.65 mg g^{-1} was attained when 2 g L^{-1} of OPL$_{LA}$ was used.

The increase in active sites led to a higher removal percentage but lowered the crude oil uptake per unit of adsorbent. This is due to the greater number of active sites available on the surface of the OPL$_{LA}$ for crude oil to be adsorbed at a higher the dosage of OPL$_{LA}$ [29], thus leading to a higher interaction between crude oil particles and adsorbent. Meanwhile, the decrease in adsorption uptake is basically due to the higher unsaturated adsorption sites during adsorption reaction [30].

3.6. Equilibrium isotherms

Adsorption isotherm is important to describe the interactions between the solute and the adsorbent. For this purpose, the effect of the initial concentration of oil adsorbed onto OPL$_{LA}$ was studied at different initial oil concentrations ranging from 400 to 6400 mg L^{-1}. As shown in Fig. 9, the adsorption uptake increased with increasing initial concentration and reached its equilibrium stage at the initial concentration up to 5600 mg L^{-1}. This result may be due to the saturation of the active sites on the OPL$_{LA}$. A smaller number of hydrocarbon molecules at a lower concentration have sufficient available adsorption sites to be adsorbed on the OPL$_{LA}$. Therefore, oil at lower concentrations resulted in a lower
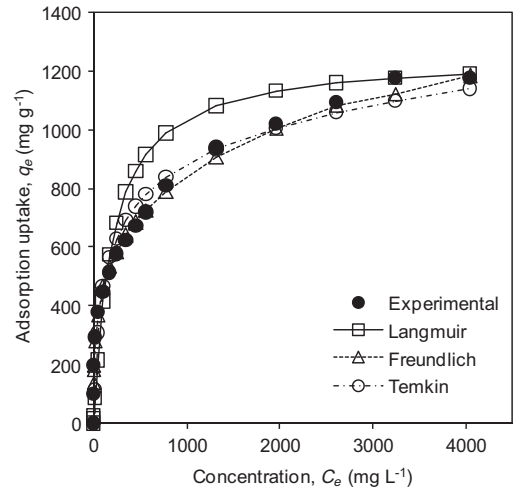
adsorption uptake of the crude oil due to the excess of the unsaturated adsorption sites.

In this study, three commonly used isotherms, the Langmuir [30], the Freundlich [31] and the Temkin [32], were employed and their non-linear form can be represented by the following equations, respectively:

$$q_e = \frac{q_m K_a C_e}{1 + K_a C_e} \tag{4}$$

$$q_e = K_F C_e^{1/n} \tag{5}$$

$$q_e = B \ln(A C_e) \tag{6}$$

where q_e (mg g^{-1}) is the amount of oil adsorbed at the equilibrium time, C_e (mg L^{-1}) is the equilibrium concentration of oil, K_L (L mg^{-1}) and q_m (mg g^{-1}) are the Langmuir adsorption constant and the theoretical maximum adsorption capacity, respectively. The K_F and n are the Freundlich constants, which indicate the extent of the adsorption and the degree of nonlinearity between the solution concentration and the adsorption, respectively while A and B are the Temkin constants. The isotherms fitting for Langmuir, Freundlich and Temkin of the adsorption of crude oil onto OPL$_{LA}$ were also shown in Fig. 9.

The applicability of the studied experimental data in fitting the equation isotherm models were determined by regression coefficient, R^2 and error function. Marquadt's percent standard deviation was employed as the error function and is given as below:

$$MPSD = 100 \times \left(\sqrt{\frac{1}{p-n} \sum_{i=1}^{p} \left[\frac{(q_{e,meas} - q_{e,cal})}{q_{e,meas}} \right]_i^2} \right) \tag{7}$$

where p is the number of experiments and n is the number of parameters of a model equation. The adsorption capacity obtained from the experimental data and calculated from the modeled equation were denoted by q_e and $q_{e,calc}$, respectively. In the error estimation, the lower the MPSD value indicates better fit of the isotherm equations [26].

All of the coefficients and MPSD error values for these three isotherm models are listed in Table 1. The result shows a good fit of the Langmuir isotherm to the experimental data with R^2 value of 0.967, suggesting the formation of monolayer coverage of crude oil onto the homogenous distribution of active sites on the OPL$_{LA}$ surface [32]. However, the higher accuracy ($R^2 = 0.995$) revealed that the Freundlich isotherm model better described the adsorp-

Table 1
Coefficients and MPSD error values of the Langmuir, Freundlich and Temkin isotherms.

Isotherm	Parameters	Values
Langmuir	q_m (mg g^{-1})	1.95
	K_L (L mg^{-1})	0.156
	R^2	0.967
	MPSD	45.27
Freundlich	K_F (mg g^{-1}) (L mg^{-1})$^{1/n}$	1.72
	n	1.39
	R^2	0.995
	MPSD	3.17
Temkin	A (1 g^{-1})	0.007
	B	334
	R^2	0.942
	MPSD	21.42

tion of crude oil onto OPL$_{LA}$. In addition, the lowest MPSD value further confirmed the suitability of the Freundlich model in describing the equilibrium data. These results demonstrated the adsorption of crude oil onto OPL$_{LA}$ takes place through multilayer adsorption process with the heterogeneous adsorption sites on the solid's surface [33]. The K_F value was 1.72. In general, as the K_F value increases, the adsorption capacity of the adsorbent for a given adsorbate also increases. According to literature, the adsorption is favorable when $1 < n < 10$, and the higher the n value, the stronger the adsorption intensity [34]. The value of n was greater than unity ($n = 1.39$), which indicates that the oil is favorably adsorbed on OPL$_{LA}$. In contrary, lower correlation coefficient of the Temkin model was observed ($R^2 = 0.942$), which indicated unsatisfactory fitting between the experimental data and isotherm equation.

3.7. Adsorption kinetics

Time of contact between adsorbate and adsorbent is of great importance in adsorption, because it depends on the nature of the system used [35]. From Fig. 10, it was observed that the crude oil uptake was rapid for the first 10 min, and thereafter proceeded at a slower rate and finally attained saturation. The initially high rate of crude oil uptake may be attributed to the existence of bare surface of active sites on OPL$_{LA}$. It was noticed that as the time was prolonged from 10 to 40 min, the adsorption uptake was increased. This is probably due to the breakage of crude oil droplets which were enhanced and thus reduced the diameter of the crude oil
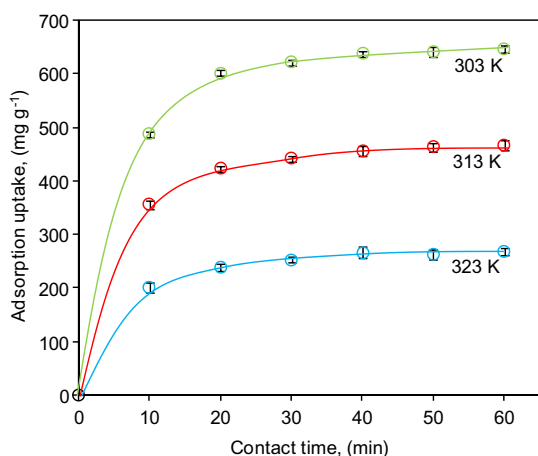

Fig. 10. Effect of contact times of adsorption of crude oil onto OPL$_{LA}$ at different adsorption temperatures. (pH 7, 2400 mg L^{-1} exposed oil, 2 g L^{-1} OPL$_{LA}$).

droplets causing more interfacial area for the adsorption to happen [36]. After 50 min, the adsorption rate was remained constant with time, presumably due to the saturation of OPL$_{LA}$ surfaces with crude oil particles as well as the equilibrium between adsorption and desorption process that occurred after the saturation [37]. However, the experimental data were measured at 60 min to be sure that full equilibrium was attained. It is seen that nearly 20 min is required for the adsorption to start at a very slow rate until the changes in adsorption uptake can be negligible relative to contact time needed. Therefore, under this effect of contact time, we chose 20 min as the optimum contact time to be used in further study.

The study of adsorption kinetics is important in the treatment of aqueous effluent because it provides valuable information on the mechanism of the adsorption process. Two well-known models of pseudo-first-order [38] and pseudo-second-order [39] were used to find the possible rate-controlling steps involved in the adsorption of crude oil, which can be expressed in the linear form as the following equations, respectively:

$$\log(q_e - q_t) = \log q_e - \frac{k_1 t}{2.303} \tag{8}$$

$$\frac{t}{q_t} = \frac{1}{k_2 q_e^2} + \frac{t}{q_e} \tag{9}$$

where q_e (mg g^{-1}) and q_t (mg g^{-1}) refer to the amount of oil adsorbed at equilibrium and at any time, t (min), respectively, and k_1 (g mg^{-1} min^{-1}) and k_2 (g mg^{-1} min^{-1}) are the rate constant of the pseudo-first-order and pseudo-second-order adsorption, respectively. The linear regression coefficient, R^2 and parameters of kinetics models were calculated and listed in Table 2. The results reveal a good fit in pseudo-second order model with the R^2 values higher than 0.997 and the approximation of experimental $q_{e,exp}$ and theoretical $q_{2e,calc}$ values at the chosen temperature compared to the pseudo-second order model. Clearly, the adsorption behaviors of crude oil on OPL$_{LA}$ do not follow the pseudo-first-order kinetics model but predominantly fit the pseudo-second-order kinetics model.

At the present time, the model of Boyd [40] is widely used for studying the mechanism of adsorption. Boyd model determines whether the main resistance to mass transfer is in the thin film (boundary layer) surrounding the adsorbent particle, or in the resistance to diffusion inside the pores. This model is expressed as:

$$F = 1 - \frac{6}{\pi^2} \sum_{n=1}^{\infty} \frac{1}{n^2} \exp(-n^2 B_t) \tag{10}$$

where F is the fractional attainment of equilibrium, at different times, t, and B_t is a function of F.

$$F = \frac{q_e}{q_t} \tag{11}$$

The values of B_t for each fraction adsorbed can be calculated by the integration of Eq. (6) proposed by Reichenberg [41] in the following approximations:
for F values >0.85,

$$B_t = -0.4977 - \ln(1 - F) \tag{12}$$

for F values <0.85,

$$B_t = \left(\sqrt{\pi} - \sqrt{\pi - \left(\frac{\pi^2 F}{3} \right)} \right)^2 \tag{13}$$

The linearity test of B_t vs. time were used to distinguish between the film- and particle-diffusion controlled adsorption. If the plot is a straight line passing through the origin, the adsorption rate was governed by the particle diffusion; otherwise it was gov-

Table 2
Coefficients of pseudo-first-order and pseudo-second-order adsorption kinetics models.

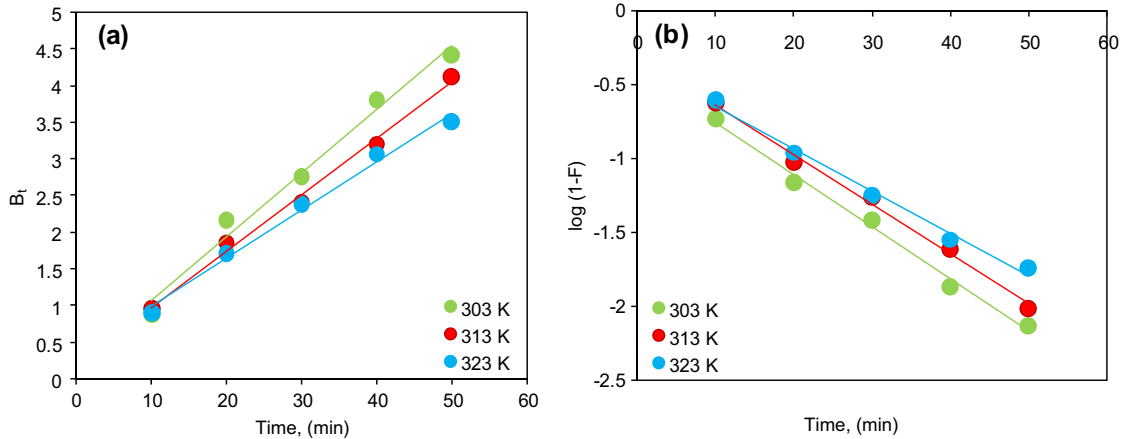| Temperature (K)	$q_{e.exp}$ (mg g^{-1})	Pseudo-first order			Pseudo-second order		
		$k_1 \times 10^{-2}$ (g mg^{-1} min^{-1})	$q_{1e.calc}$ (mg g^{-1})	R^2	$k_2 \times 10^{-3}$ (g mg^{-1} min^{-1})	$q_{2e.calc}$ (mg g^{-1})	R^2
303	645.73 ± 6.65	10.02	488	0.986	0.900	667	0.998
313	467.58 ± 9.88	9.35	376	0.982	1.10	476	0.998
323	268.61 ± 6.53	8.36	200	0.975	1.70	278	0.997

Fig. 11. Boyd plots for the adsorption of crude oil onto OPL$_{LA}$ at different adsorption temperatures.

Table 3
Thermodynamics parameters for the adsorption of oil onto OPL$_{LA}$.

Temperature (K)	q_e (mg g^{-1})	ΔG^o (kJ mol^{-1})	ΔH^o (kJ mol^{-1})	ΔS^o (kJ mol^{-1} K^{-1})	E_a (kJ mol^{-1})
303	1179 ± 12.92	0.804			
313	706.83 ± 24.96	2.824	−38.3	−0.228	25.8
323	333.67 ± 17.00	5.372			

Table 4
Comparison of oil adsorption capacity of various adsorbents.

Sorbent	Adsorption capacity (g g^{-1})	pH	Oil conc. (mg L^{-1})	Temperature (°C)	Contact time (min)	Ref.
Lauric acid treated oil palm leaves (OPL$_{LA}$)	1.2 ± 0.12	7	5600	303	20	This study
Hydrophobized vermiculite with carnauba wax	1.1 ± 0.1	–	50	–	60	[5]
Hydrophobic aquaphyte – *Salvinia* sp. (HAS)	1.39	–	586	298	180	[6]
Hydrogel of chitosan based on polyacrylamide (HCP)	2.30	3	3000	298	200	[7]
Hydrophobic aerogel (HA)	2.80	–	1000	298	>180	[2]
Carbonized rice husks (CRH)	6.00	7.0	–	298	10	[8]
Black rice husk ash (BHRA)	6.22	–	–	293	3	[9]
Oleic acid-grafted sawdust (OGSD)	6.00	5.19	8000	298	5	[10]
Recycled wool-based nonwoven material (RNWM)	11.50	–	80,000	–	10	[11]

erned by the film diffusion [42]. Fig. 11a shows the Boyd plot for the crude oil adsorption on OPL$_{LA}$. The plots for all the temperatures are linear, but they do not pass the origin, indicating the film-diffusion-controlled mechanism. To reconfirm the above observation, log (1-F) vs. time was plotted at different temperatures and the straight lines deviating from the origin were obtained for all plots as shown in Fig. 11b. These observations further support the fact that the adsorption of crude oil onto OPL$_{LA}$ occurs via internal transport mechanism at all the temperatures studied [43].

3.8. Thermodynamics studies

Thermodynamics parameters were evaluated to confirm the nature of the adsorption. The effect of temperature on the adsorp-

tion of oil onto OPL$_{LA}$ was evaluated over the temperature range of 303–323 K. As shown in Table 3, the adsorption uptake of the oil increased with decreasing temperature, which indicates that the process was exothermic [44].

The free energy change (ΔG^o) was calculated by the following equation:

$$\Delta G^O = -RT \ln K_C \tag{14}$$

where K_c is the equilibrium constant of the adsorption, which was obtained from the following equation:

$$K_C = \frac{C_e(adsorbent)}{C_e(solution)} \tag{15}$$

where C_e (adsorbent) and C_e (mixture) are the equilibrium concentrations of the oil molecules on the adsorbent and in mixture,

respectively. The values of the enthalpy change (ΔH^o) and the entropy change (ΔS^o) could be determined from the van't Hoff equation:

$$\ln K_C = \frac{\Delta S^O}{R} - \frac{\Delta H^O}{RT} \tag{16}$$

The values of these thermodynamics parameters determined at three different temperatures are listed in Table 3. The increase in the ΔG^o values with increasing temperature indicates a decrease in the feasibility and spontaneity of the adsorption at higher temperatures [45]. The negative ΔH^o value suggests that the crude oil adsorption may represent an exothermic process [42]. In general, the magnitude of the enthalpy is about 20–40 kJ mol^{-1} for physisorption and 80–400 kJ mol^{-1} for chemisorption [46]. Therefore, this adsorption of crude oil onto OPL$_{LA}$ may classify as physisorption since its absolute magnitude of enthalpy is 38.3 kJ mol^{-1}, which is in the physisorption range. The negative value of ΔS^o suggests that there is a decrease in randomness at the solid–mixture interface during the adsorption of crude oil from water due to the highly ordered crude oil molecules in the hydrophobic layer of OPL$_{LA}$ at adsorption equilibrium [47].

The activation energy, E_a, is defined as the minimum kinetics energy needed by the sorbate molecules to react with the active sites available on the surface of the adsorbent [48]. The value of E_a can be obtained by the Arrhenius equation by calculating the slope of the plot of $\ln k_2$ vs. $1/T$:

$$\ln k_2 = \ln A - \frac{E_a}{R}\left(\frac{1}{T}\right) \tag{17}$$

where R (8.314 J mol^{-1} K^{-1}) is the gas constant. The slope of the plot of $\ln k_2$ vs. $1/T$ gives a value of the activation energy (E_a) of 25.8 kJ mol^{-1} (Table 3). This value is showing that the presence of low energy barrier to initiate the reaction and implied that the adsorption of crude oil onto OPL$_{LA}$ is a physical adsorption. The value is consistent with the fact that the magnitude of the activation energy for physical adsorption is usually between 5 and 40 kJ mol^{-1} [49]. These results were also consistent with the value of enthalpy in Table 3, which indicates the crude oil adsorption on OPL$_{LA}$ was took place via physical adsorption.

3.9. Comparison of oil adsorption capacity of OPL$_{LA}$ with various adsorbents

Table 4 lists the comparison of maximum adsorption capacity of crude oil on various adsorbents. It was observed that OPL$_{LA}$ is comparable to that of hydrophobized vermiculite with carnauba wax [5] and hydrophobic aquaphyte (HAS) [6] but its adsorption capacity was slightly lower than hydrogel of chitosan based on polyacrylamide (HCP) [7] and hydrophobic aerogel (HA) [2]. Carbonized rice husks (CRH) [8], black rice husk ash (BHRA) [9] and oleic acid-grafted sawdust (OGSD) [10] gave five times higher adsorption capacity compared to OPL$_{LA}$ and recycle wool non-woven material (RWNM) [11] posses the highest adsorption capacity. Generally, it could be dictated that the hydrophobicity and surface area play an important role in the enhancement of oil sorption. Modifications of the adsorbents by acrylamide (HCP), trimethylsilyl (HA) and fatty acid groups (OGSD) enhanced their hydrophobicity, thus allow more oil to be attracted to their surface. The hydrophobicity could be also improved by pyrolysis, which provides moisture and volatile components on the surface of the adsorbent (CRH and BHRA). On the other hand, higher surface area posses by certain adsorbents either by their natural structure (HAS) or modification (RWNM) were also responsible for increasing the capability of trapping oil. The pyrolysis on the preparation of RWNM resulted in fiber splitting and fibrillation for enhancement of the specific surface area.

4. Conclusions

In conclusion, OPL$_{LA}$ shows the potential to be a crude-oil adsorbent in oily water. The advantage of using OPL as an adsorbent in this study is that its economical and solving environmental problems due to the abundance of OPL in South East region, especially Malaysia and Indonesia. The successful impregnation of lauric acid into OPL was supported by all the analysis studied. Pretreatment of the raw OPL by lauric acid was effectively enhanced its surface hydrophobicity, thus increased the adsorption capacity. FTIR analysis, BET analysis and FE-SEM micrographs have elucidated the significant uptake of crude oil from the water onto OPL$_{LA}$. The adsorption of crude oil onto OPL$_{LA}$ exhibits pseudo-second-order kinetics, and the adsorption was controlled by film-diffusion and governed by the internal transport mechanism. All of the experimental data fit well with the Freundlich model. The thermodynamics studies presented here prove the feasibility, spontaneity and exothermic nature of the adsorption, which is controlled by a physisorption process.

References

[1] T.T. Lim, X. Huang, Evaluation of kapok (Ceiba pentandra (L.) Gaertn) as a natural hollow hydrophobic–oleophilic fibrous sorbent for oil spill cleanup, Chemosphere 66 (2007) 955–963.
[2] D. Wang, T. Silbaugh, R. Pfeffer, Y.S. Lin, Removal of emulsified oil from water by inverse fluidization of hydrophobic aerogels, Powder Technol. 203 (2010) 298–309.
[3] S. Syed, M.I. Alhazzaa, M. Asif, Treatment of oily water using hydrophobic nano-silica, Chem. Eng. J. 167 (2011) 99–103.
[4] O.K. Karaksi, A. Moutsatsou, Surface modification of high calcium fly ash for its application in oil spill clean-up, Fuel 89 (2010) 3966–3970.
[5] U.G. Da Silva, M.A.F. Melo, A.F. de Silva, R.A. Farias, Adsorption of crude oil on anhydrous and hydrophobized vermiculite, J. Colloid Interf. Sci. 260 (2003) 302–304.
[6] T.H. Ribeiro, J. Rubio, R.W. Smith, A dried hydrophobic aquaphyte as an oil filter for oil/water emulsions, Spill Sci. Technol. Bull. 8 (2003) 483–489.
[7] H.H. Sokker, N.M. El-Sawy, M.A. Hassan, B.E. Al-Anadouli, Adsorption of crude oil from aqueous solution by hydrogel of chitosan based polyacrylamide prepared by radiation induced graft polymerization, J. Hazard. Mater. 190 (2011) 359–365.
[8] D. Angelova, I. Usunov, S. Uzunova, A. Gigova, L. Minchev, Kinetics of oil and oil products adsorption by carbonized rice husks, Chem. Eng. J. 172 (2011) 306–311.
[9] L. Vlaev, P. Petkov, A. Dimitrov, S. Genieva, Cleanup of water polluted with crude oil or diesel fuel using rice husks ash, J. Taiwan Inst. Chem. Eng 42 (2011) 957–964.
[10] S.S. Banerjee, M.V. Joshi, R.V. Jayaram, Treatment of oil spill by sorption technique using fatty acid grafted sawdust, Chemosphere 64 (2006) 1026–1031.
[11] M.M. Radetic, D.M. Jocic, P.M. Jovancic, Z.L.J. Petrovic, H.F. Thomas, Recycled wool based non-woven material as an oil sorbent, Environ. Sci. Technol. 37 (2003) 1008–1012.
[12] S. Sumathi, S.P. Chai, R. Mohamed, Utilization of oil palm as a source of renewable energy in Malaysia, J. Renew. Sust. Energy Rev. 12 (2008) 2404–2421.
[13] R. Hashim, N. Saari, O. Sulaiman, T. Sugimoto, S. Hiziroglu, M. Sato, R. Tanaka, Effect of particle geometry on the properties of binderless particleboard manufactured from oil palm trunk, Mater. Des. 31 (2010) 4251–4257.
[14] R. Hashim, W.N.A.W. Nadhari, O. Sulaiman, F. Kawamura, S. Hiziroglu, M. Sato, T. Sugimoto, T.G. Seng, R. Tanaka, Characterization of raw materials and manufactured binderless particleboard from oil palm biomass, Mater. Des. 32 (2011) 246–254.
[15] J. Mao, S.W. Won, S.B. Choi, M.W. Lee, Y.S. Yun, Surface modification of the Corynebacterium glutamicum biomass to increase carboxyl binding site for basic dyes molecules, Biochem. Eng. J. 49 (2009) 1–6.

[16] G.F. Fanta, T.P. Abbort, R.C. Burr, W.M. Doane, Ion exchange reactions of quaternary ammonium halides with wheat straw. Preparations of oil-adsorbents, Carbohydr. Polym. 7 (1987) 97–109.

[17] C. Teas, S. Kalligeros, F. Zanikos, S. Stournas, E. Lois, G. Anastopoulos, Investigation of the effectiveness of absorbent materials in oil spills clean up, Desalination 140 (2001) 259–264.

[18] A.B.P. Marin, J.F. Ortuno, M.I. Aguilar, V.S. Meseguer, J. Saez, M. Llorens, Use of chemical modification to determine the binding of Cd(II), Zn(II) and Cr(III) ions by orange waste, Biochem. Eng. J. 53 (2010) 2–6.

[19] H. Yang, R. Yan, H. Chen, D.H. Lee, C. Zheng, Characteristics of hemicelluloses, cellulose, and lignin pyrolysis, Fuel 86 (2007) 1781–1788.

[20] K.K. Pandey, A.J. Pitman, FTIR studies of the changes in wood chemistry following decay by brown-rot and white-rot fungi, Int. Biodeterior. Biodegrad. 52 (2003) 151–160.

[21] K.Y. Foo, B.H. Hameed, Textural porosity, surface chemistry and adsorptive properties of durian shell derived activated carbon prepared by microwave assisted NaOH activation, Chem. Eng. J. 184 (2012) 57–65.

[22] A. Shahsavand, M.N. Shahrak, Reliable prediction of pore size distribution for nano-sized adsorbents with minimum information requirements, Chem. Eng. J. 171 (2011) 69–80.

[23] P. Schatzerg, Investigations of sorbents for removing oil spills from water. US Coast Guard Report. No. 724110.1/2/1, US Coast Guard Headquaters, Washington, DC, 1971.

[24] Q.F. Wei, R.R. Mather, A.F. Fortheringham, Oil removal from used sorbents using a biosurfactant, Bioresour. Technol. 96 (2005) 331–334.

[25] R. Gong, Y. Jin, F. Chen, Z. Liu, Enhanced malachite green removal from aqueous solution by citric acid modified rice straw, J. Hazard. Mater. 137 (2006) 865–870.

[26] S. Ibrahim, S. Wang, H.M. Ang, Removal of emulsified oil from oily wastewater using agricultural waste barley straw, Biochem. Eng. J. 49 (2010) 78–83.

[27] J.Y. Farah, N.S. El-Gendy, L.A. Farahat, Biosorption of astrazone blue basic dye from an aqueous solution using dried biomass of Baker's yeast, J. Hazard. Mater. 148 (2007) 402–408.

[28] A.L. Ahmad, S. Bhatia, N. Ibrahim, S. Sumathi, Adsorption of residual oil from palm oil mill effluent using rubber powder, Braz. J. Chem. Eng. 22 (2005) 371–379.

[29] V.O. Arief, K. Trilestari, J. Sunarso, N. Indraswati, S. Ismadji, Recent progress on biosorption of heavy metals from liquid using low cost biosorbents: characterization, biosorption parameters and mechanism studies, CLEAN-Soil Air Water 36 (2008) 937–962.

[30] W.S. Wan Ngah, M.A.K.M. Hanafiah, Biosorption of copper ions from dilute aqueous solution on base treatedrubber (*Hevea brasiliensis*) leaves powder: kinetics, isotherm, and biosorption mechanism, J. Environ. Sci. 20 (2008) 1168–1176.

[31] H.M.F. Freundlich, Über die adsorption in lösungen, Z. Phys. Chem. 57 (1906) 385–470.

[32] B.H. Hameed, Removal of cationic dye from aqueous solution using jackfruit peels as non-conventional low-cost adsorbent, J. Hazard. Mater. 162 (2009) 344–350.

[33] K. Gobi, M.D. Mashitah, V.M. Vadivelu, Adsorptive removal of Methylene Blue using novel adsorbent from palm oil mill effluent waste activated sludge: equilibrium, thermodynamics and kinetics studies, Chem. Eng. J. 171 (2011) 1246–1252.

[34] Q.-S. Liu, T. Zheng, P. Wang, J.-P. Jiang, N. Li, Adsorption isotherm, kinetics and mechanism studies of some substituted phenols on activated carbon fibers, Chem. Eng. J. 157 (2010) 348–356.

[35] Z. Baysal, E. Cinar, Y. Bulut, H. Alkan, M. Dogru, Equilibrium and thermodynamics studies on biosorption of Pb(II) onto *Candida albicans* biomass, J. Hazard. Mater. 161 (2009) 62–67.

[36] S. Micheal, K. Heike, S. Helmar, Adsorption kinetics of emulsifiers at oil-water interfaces and their effect on mechanical emulsification, Chem. Eng. Process. 33 (1994) 307–311.

[37] M.E. Argun, S. Dursun, M. Karatas, M. Guru, Activation of pine cone using Fenton oxidation for Cd(II) and Pb(II) removal, Bioresour. Technol. 99 (2008) 8691–8698.

[38] S. Lagergren, B.K. Svenska, Zur theorie der sogennantan adsorption geloester stoffe, Veternskapsakad Handl. 24 (1898) 1–39.

[39] Y.S. Ho, G. McKay, Pseudo-second order model for sorption processes, Process Biochem. 34 (1999) 451–465.

[40] G.E. Boyd, A.W. Adamson, L.S. Myers Jr., The exchange adsorption of ions from aqueous solution by organic zeolites. Part II. Kinetics, J. Am. Chem. Soc. 69 (1947) 2836–2848.

[41] D. Reichenberg, Properties of ion exchange resins in relation to their structure. Part III. Kinetics of exchange, J. Am. Chem. Soc. 75 (1953) 589–598.

[42] B.H. Hameed, M.I. El-Khaiary, Malachite green adsorption by rattan sawdust: isotherm, kinetics and mechanism modeling, J. Hazard. Mater. 162 (2009) 344–350.

[43] R. Ahmad, R. Kumar, Adsorption studies of hazardous malachite green onto treated ginger waste, J. Environ. Manage. 91 (2010) 1032–1038.

[44] A.A. Jalil, S. Triwahyono, S.H. Adam, N.D. Rahim, M.A.A. Aziz, N.H.H. Hairom, N.A.M. Razali, M.A.Z. Abidin, M.K.A. Mohamadiah, J. Hazard. Mater. 181 (2010) 755–762.

[45] M. Auta, B.H. Hameed, Preparation of waste tea activated carbon using potassium acetate as an activating agent for adsorption of Acid Blue 25 dye, Chem. Eng. J. 171 (2011) 502–509.

[46] M.A.Z. Abidin, A.A. Jalil, S. Triwahyono, S.H. Adam, N.H.N. Kamarudin, Recovery of gold(III) from an aqueous solution onto a *Durio zibethinus* husk, Biochem. Eng. J. 54 (2011) 124–131.

[47] D. Bera, D. Lahiri, A. Nag, Kinetics study on bleaching of edible oil using charred sawdust as a new adsorbent, J. Food Eng. 65 (2004) 33–36.

[48] L.G. Wade, Organic Chemistry, Pearson Education International, United States of America, 2006.

[49] Q. Li, L. Chai, Z. Yang, Q. Wang, Kinetics and thermodynamics of Pb(II) adsorption onto modified spent grain from aqueous solutions, Appl. Surf. Sci. 255 (2009) 4298–4303.